

Supporting information

A novel solvent mixing method for the preparation of polymer/inorgano-layered double hydroxides nanocomposites

Qiang Wang^a, Xi Zhang^b, Jiahua Zhu^b, Zhanhu Guo^b and Dermot O'Hare^{*a}

^aChemistry Research Laboratory, Department of Chemistry, University of Oxford, 12 Mansfield Road, Oxford, OX1 3TA, UK

^bIntegrated Composites Laboratory, Dan F Smith Department of Chemical Engineering, Lamar University, Beaumont, TX 77710, USA

CONTENTS

1. Experimental Details and Characterising Data

Table S1. All solvents that can modify LDH nanoparticles and lead to stable LDH suspensions in xylene solvent.

Table S2. Alkanes, alcohols, ethers, and ketones that have been examined as dispersing solvents for modified LDH nanoparticles.

Table S3. Aromatic solvents that have been examined as dispersing solvents for modified LDH nanoparticles.

Table S4. Comparison of the temperature increase in $T_{0.5}$ for PP/LDH nanocomposites reported in literature and our result.

Table S5. Summary of recrystallisation temperature (T_c), ΔH_c , melting temperature (T_m), and ΔH_m as measured by DSC for PP/Mg₃Al-LDH nanocomposites.

Figure S1. (a) Mg₃Al-CO₃ LDH nanoparticles dispersed in H₂O, (b) dried Mg₃Al-CO₃ LDH.

Figure S2. The absorbance at 317 nm as a function of LDH concentration for the LDH/xylene suspensions.

Figure S3. XRD patterns of Mg₃Al-CO₃ LDHs after wash with water or acetone (★) sample holder.

Figure S4. Dynamic light scattering analysis of Mg₃Al-CO₃ LDH nanoparticles dispersed in xylene and water.

Figure S5. XRD data for pure PP, pure Mg₃Al-CO₃ LDH, and PP/Mg₃Al-LDH nanocomposites with different LDH loadings.

Figure S6. (a) SEM image, (b) Mg mapping, and (c) Al mapping of 6 wt% PP/Mg₃Al-CO₃ nanocomposite.

Figure S7. (a) Storage modulus (G') as a function of frequency for PP/Mg₃Al LDH nanocomposites. (b) Mechanical loss factor ($\tan \delta$) of as a function of frequency for PP/Mg₃Al-LDH nanocomposites.

Figure S8. XRD analyses of pure PP, PP/Mg₃Al-Cl, PP/Mg₃Al-NO₃, PP/Mg₃Al-CO₃ nanocomposites; (▼) LDH.

Figure 9. XRD analyses of pure PP, PP/Ca₂Al-NO₃ nanocomposite, and pure Ca₂Al-NO₃ LDH.

Figure S10. TGA analysis of Pure PP, PP/Mg₃Al-CO₃, PP/Mg₃Al-Cl, PP/Mg₃Al-NO₃, and PP/Ca₂Al-NO₃ LDH nanocomposites in air.

1. Experimental Details and Characterising Data

1.1. Synthesis of samples

Synthesis of LDHs – All LDHs were prepared using a coprecipitation method. In brief, Mg₃Al-CO₃ was prepared by adding a Mg(NO₃)₂·6H₂O and Al(NO₃)₃·9H₂O solution drop-wise into a Na₂CO₃ solution. The pH of the precipitation was controlled at ca. 12 using a NaOH solution. Mg₃Al-NO₃ was prepared by adding a Mg(NO₃)₂·6H₂O and Al(NO₃)₃·9H₂O solution drop-wise into a NaNO₃ solution. The pH of the precipitation was controlled at ca. 10 using a NaOH solution. Mg₃Al-Cl was prepared by adding a MgCl₂ and AlCl₃·xH₂O solution into a NaCl solution, with the pH controlled at ca. 10 using a NaOH solution. Ca₂Al-NO₃ was prepared by adding a Ca(NO₃)₂·4H₂O and Al(NO₃)₃·9H₂O solution drop-wise into a NaNO₃ solution. The pH of the precipitation was controlled at ca. 10 using a NaOH solution. All prepared LDH samples were aged at room temperature for 24 h with continuous stirring. After aging, LDH nanoparticles were separated by centrifuge (3750 rpm) and

washed with deionized (DI) water until pH close to 7. Then the LDH slurries were washed subsequently with H₂O/ethanol (1:1) for 3 times, and acetone for 3 times. After washing, the obtained LDH slurries were directly used for the preparation of PP/LDH nanocomposites without drying.

Synthesis of PP/LDH nanocomposites – 5 g PP, the LDH slurry prepared above and 100 ml xylene were charged into a 250 ml round bottom flask. The amount of LDH added to PP corresponds to 1, 3, 6, 9, and 12 wt%, respectively. The mixture was refluxed at approximately 140 °C for 2 h. After the reflux process was finished, the hot xylene solution containing dissolved PP and highly dispersed LDH nanoparticles was poured into 100 ml hexane (also called a solvent extraction method). The obtained PP/LDH nanocomposites were collected by filtration and dried in vacuum.

1.2.Characterization of samples

X-ray diffraction (XRD) – XRD patterns were recorded on a PANalytical X’Pert Pro instrument in reflection mode with Cu Ka radiation. The accelerating voltage was set at 40 kV with 40 mA current ($\lambda = 1.542\text{ \AA}$) at $0.01^\circ \text{ s}^{-1}$ from 5° to 70° with a slit size of 1/4 degree.

Transmission Electron Microscopy (TEM) – TEM analysis was performed on JEOL 2100 microscope with an accelerating voltage of 400 kV. LDH nannoparticles were dispersed in water with sonication and then cast onto copper grids coated with Formvar film.

Scanning Electron Microscopy (SEM) – SEM analysis was performed on a JEOL JSM 6100 scanning electron microscope with an accelerating voltage of 20 kV. LDHs powders were spread on carbon tape adhered to an SEM stage. Before observation, the samples were sputter coated with a thin platinum layer to prevent charging and to improve the image quality.

Dynamic light scattering (DLS) – The LDH particle size distribution in both xylene and water were characterised by dynamic light scattering measurements using a particle size analyzer (Malvern Zetasizer Nano ZS, UK) at room temperature.

Thermal stability behavior – The thermal stability of neat PP and its nanocomposites was studied by thermal gravimetric analysis (TGA, Netzsch), which was carried out with a heating rate of 10 °C/min and an air or N₂ flow rate of 20 mL/min from 25 to 600 °C.

Recrystallization and melting behavior – The recrystallization and melting behavior of neat PP and nanocomposite was measured by a TA Instrument Q200 differential scanning calorimeter (DSC). Experiments were run on samples of about 10 mg. Each sample was first heated from room temperature to 220 °C with a heating rate of 10 °C/min to remove thermal history, cooled to 40 °C at a rate of 10 °C/min, and then reheated to 220 °C at a rate of 10 °C/min to determine the melt temperature. The experiments were carried out under a nitrogen flow rate of 50 mL/min.

Rheological behavior – The rheological behavior of neat PP and nanocomposite was studied using TA Instruments AR 2000ex Rheometer. An environmental test chamber (ETC) steel parallel-plate geometry (25 mm in diameter) was used to perform the measurement at 180 °C, with dynamic oscillation frequency sweeping from 100 to 0.1 Hz in the linear viscoelastic (LVE) range (strain 1%) under a nitrogen atmosphere to prevent the oxidation of PP.

Table S1. All solvents that can modify LDH nanoparticles and lead to stable LDH suspensions in xylene solvent.

Solvents	Boiling point (°C)	Viscosity (cPoise)	P'*	Solubility in water (%w/w)
Acetone	56	0.32	5.1	100
Acetonitrile	82	0.37	5.8	100
Dimethylformamide	155	0.92	6.4	100
Dimethyl Sulfoxide	189	2	7.2	100
Dioxane	101	1.54	4.8	100
Ethanol	78	1.2	4.3	100
Methanol	65	0.6	5.1	100
n-propanol	97	2.27	4.0	100
Iso-propanol	82	2.3	3.9	100
Tetrahydrofuran	65	0.55	4.0	100

*Polarity (P') as defined in Snyder and Kirkland (Snyder, L. R.; Kirkland, J. J. In Introduction to modern liquid chromatography, 2nd ed.; John Wiley and Sons: New York, 1979; pp 248-250)

Table S2. Alkanes, alcohols, ethers, and ketones that have been examined as dispersing solvents for modified LDH nanoparticles.

Solvent groups	Solvents	Formula	P'*	Dispersion
Alkanes	Hexane	C ₆ H ₁₄	0.1	Not good
	Trimethylpentane	C ₈ H ₁₈	0.1	Not good
	Decane	C ₁₀ H ₂₂	0.3	Not good
	Dodecane	C ₁₂ H ₂₆	-	Not good
Alcohols	Methanol	CH ₃ OH	5.1	Not good
	Ethanol	C ₂ H ₅ OH	4.3	Not good
	1-Butanol	C ₄ H ₉ OH	3.9	Not good
Ethers	Dioxane	C ₄ H ₈ O ₂	4.8	Not good
	Tetrahydrofuran (THF)	C ₄ H ₈ O	4.0	Not good
	Diethyl ether	C ₄ H ₁₀ O	2.8	Not good
Ketone	Acetone	C ₃ H ₆ O	5.1	Not good

*Polarity (P') as defined in Snyder and Kirkland (Snyder, L. R.; Kirkland, J. J. In Introduction to modern liquid chromatography, 2nd ed.; John Wiley and Sons: New York, 1979; pp 248-250,)

Table S3. Aromatic solvents that have been examined as dispersing solvents for modified LDH nanoparticles.

Solvents	Formula	P'	dispersion
Benzene	C ₆ H ₆	2.7	good
Toluene	C ₆ H ₅ -CH ₃	2.4	good
Xylene	C ₆ H ₄ (CH ₃) ₂	2.5	good
Mesitylene	C ₆ H ₃ (CH ₃) ₃	-	good
Benzyl alcohol	C ₆ H ₅ CH ₂ OH	-	good
Chlorobenzene	C ₆ H ₅ Cl	2.7	good
o-Dichlorobenzene	C ₆ H ₄ Cl ₂	2.7	good
Trichlorobenzene	C ₆ H ₃ Cl ₃	-	good
Benzenesulfonyl chloride	C ₆ H ₅ SO ₂ Cl	-	Not good
Benzoyl chloride	C ₆ H ₅ COCl	-	Not good
Benzaldehyde	C ₆ H ₅ CHO	-	Not good

Polarity (P') as defined in Snyder and Kirkland (Snyder, L. R.; Kirkland, J. J. In Introduction to modern liquid chromatography, 2nd ed.; John Wiley and Sons: New York, 1979; pp 248-250.)

Table S4. Comparison of the temperature increase in $T_{0.5}$ for PP/LDH nanocomposites reported in literature and our result.

Nanocomposites	Decomposition atmosphere	$\Delta T_{0.5}$ ($^{\circ}\text{C}$)	References
PP/IFR/Mg-Al-DDS ^a	air	40–52	26
PP/Zn-Al-DDS	air	40	27
PP/Mg-Al-DBS ^b	air	37	28
PP/PP-g-MAH/Mg-Al-DDS ^c	air	48	29
PP/PP-g-MAH/Co-Al-DBS	N_2	0	30
PP/Mg-Al-CO ₃	air	44	our work
PP/Mg-Al-Cl	air	44	our work
PP/Mg-Al-NO ₃	air	30	our work
PP/Ca-Al-NO ₃	air	41	our work
PP/Mg-Al-CO ₃	N_2	11	our work

^aPP/IFR/Mg-Al-DDS: PP with an intumescent flame retardant (IFR) system of ammonium polyphosphate/pentaerythritol (APP/PER), and dodecyl sulfate intercalated Mg-Al LDH; ^bPP/Mg-Al-DBS: PP with dodecylbenzene sulfonate (DBS) intercalated Mg-Al LDH; ^cPP/PP-g-MAH/Mg-Al-DDS: PP with maleic anhydride-grafted PP (PP-g-MAH), and DDS intercalated Mg-Al LDH;

Table S5. Summary of recrystallisation temperature (T_c), ΔH_c , melting temperature (T_m), and ΔH_m as measured by DSC for PP/Mg₃Al-LDH nanocomposites.

LDH loading (wt%)	T_c ($^{\circ}\text{C}$)	ΔH_c /J g ⁻¹	T_m ($^{\circ}\text{C}$)	ΔH_m /J g ⁻¹
0	108.31	85.61	153.65	85.70

1	116.52	91.85	156.19	90.28
3	118.10	94.84	157.89	93.75
6	120.81	81.76	158.34	86.67
9	121.27	87.94	157.98	89.37
12	122.90	86.51	158.56	92.79

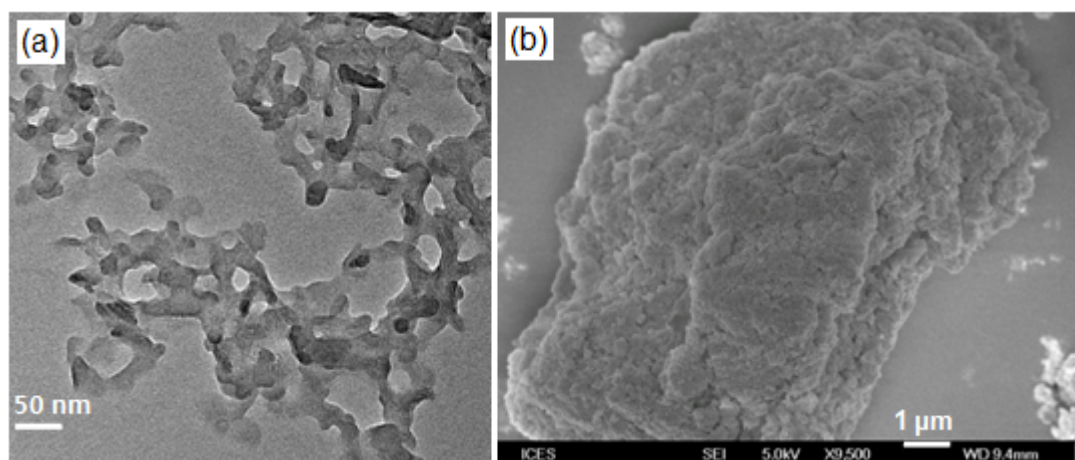


Figure S1. (a) $\text{Mg}_3\text{Al}-\text{CO}_3$ LDH nanoparticles dispersed in H_2O , (b) dried $\text{Mg}_3\text{Al}-\text{CO}_3$ LDH.

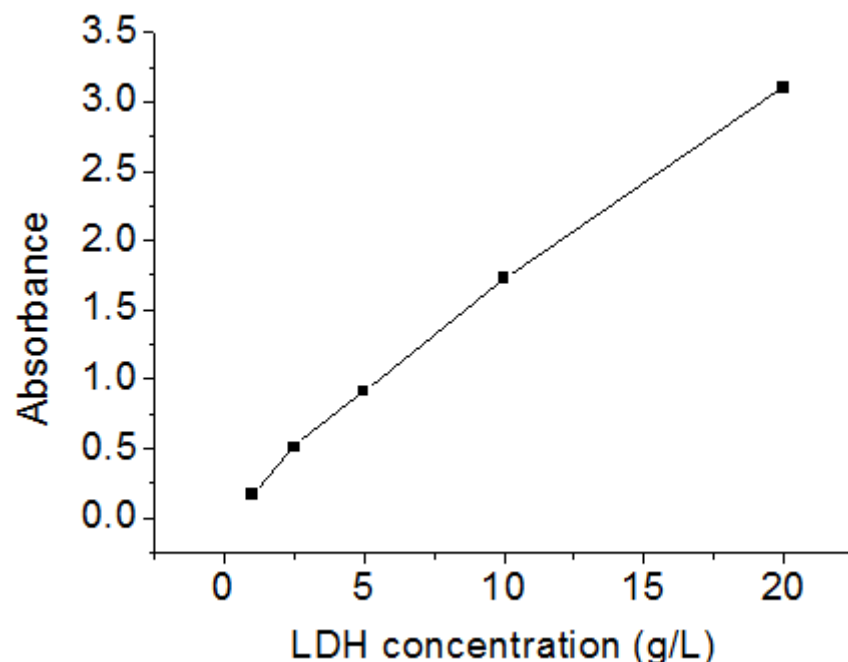


Figure S2. The absorbance at 317 nm as a function of LDH concentration for the LDH/xylene suspensions.

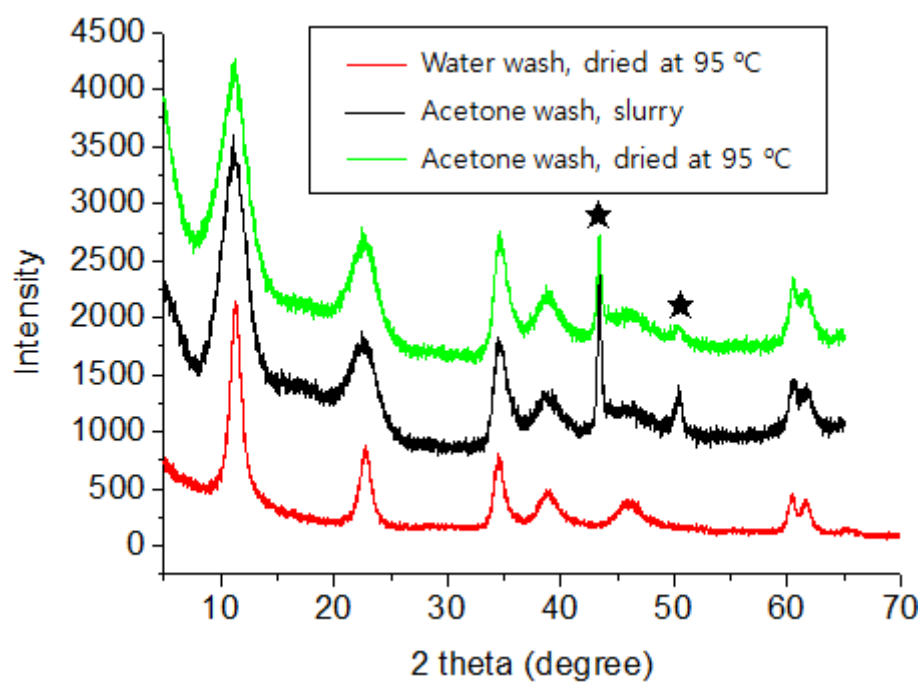


Figure S3. XRD patterns of $\text{Mg}_3\text{Al}-\text{CO}_3$ LDHs after washing with water or acetone, (★) sample holder.

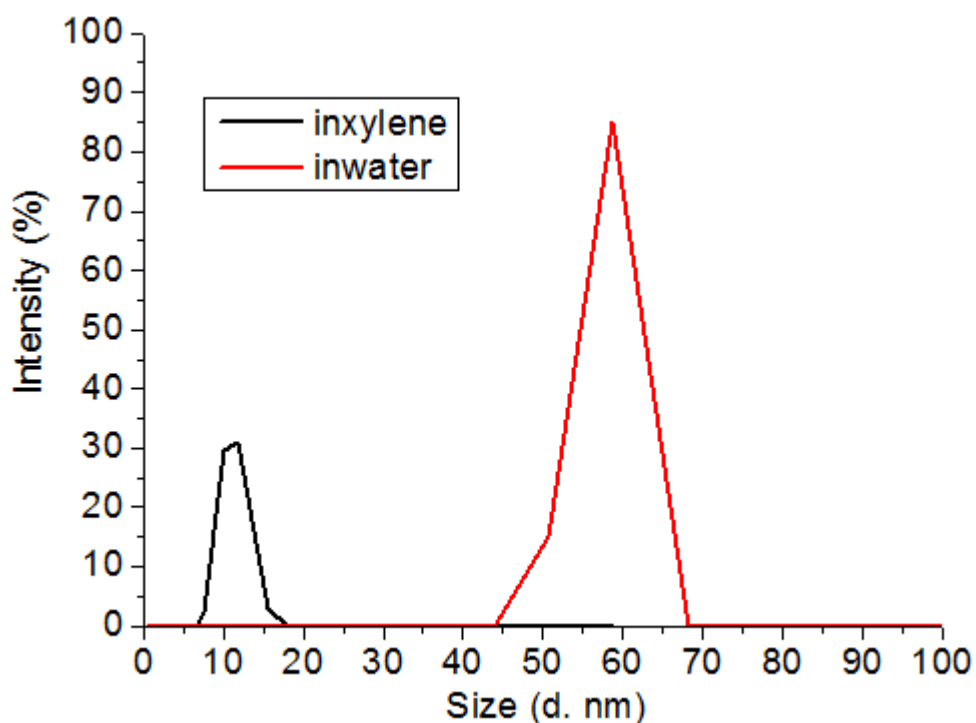


Figure S4. Dynamic light scattering analysis of Mg₃Al-CO₃ LDH nanoparticles dispersed in xylene and water.

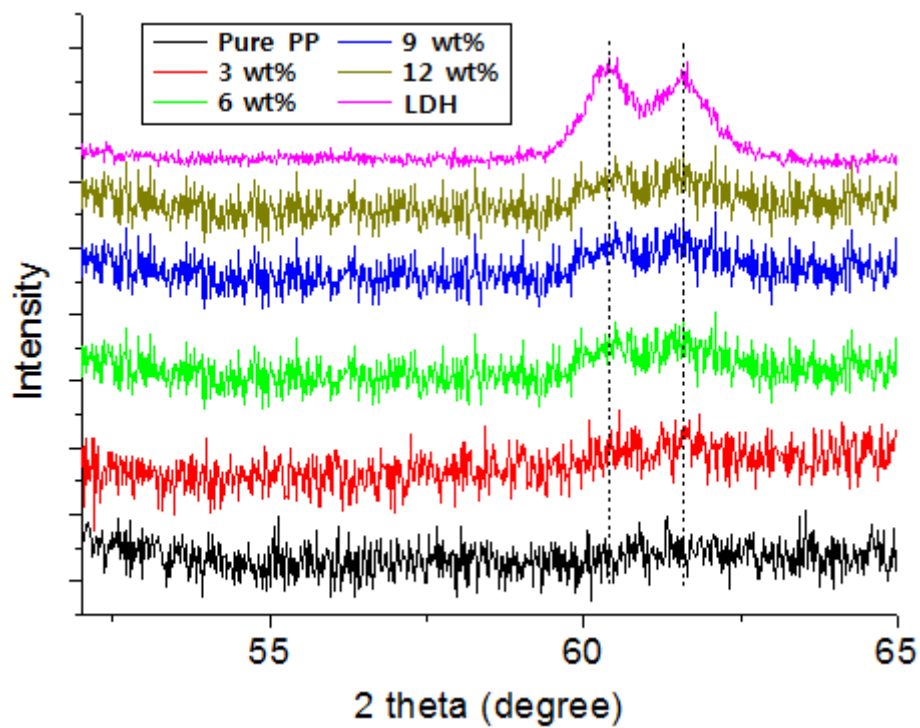


Figure S5. XRD data for pure PP, pure Mg₃Al-CO₃ LDH, and PP/Mg₃Al-LDH nanocomposites with different LDH loadings.

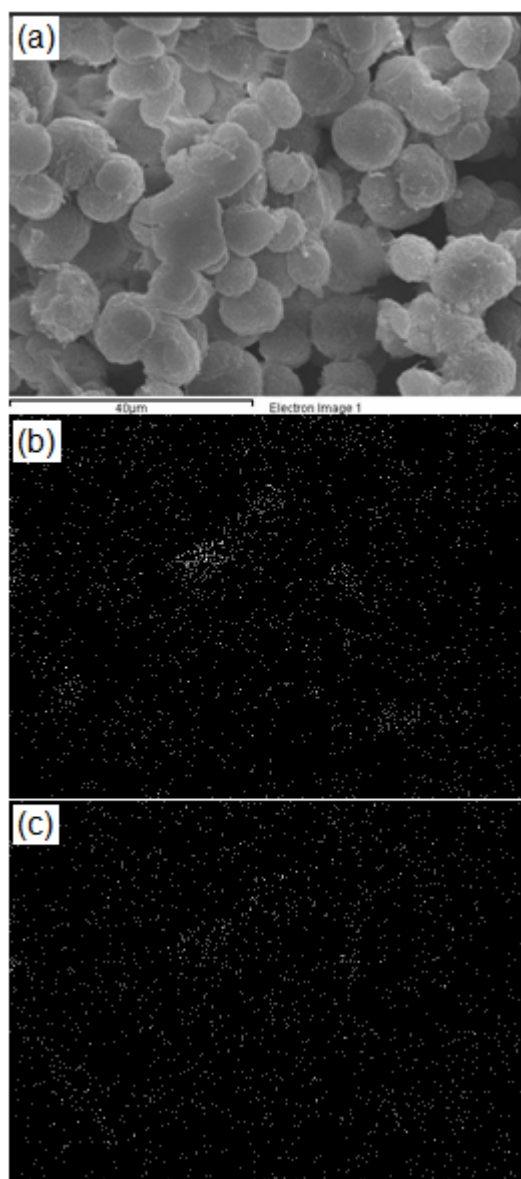


Figure S6. (a) SEM image, (b) Mg mapping, and (c) Al mapping of 6 wt% PP/Mg₃Al-CO₃ nanocomposite.

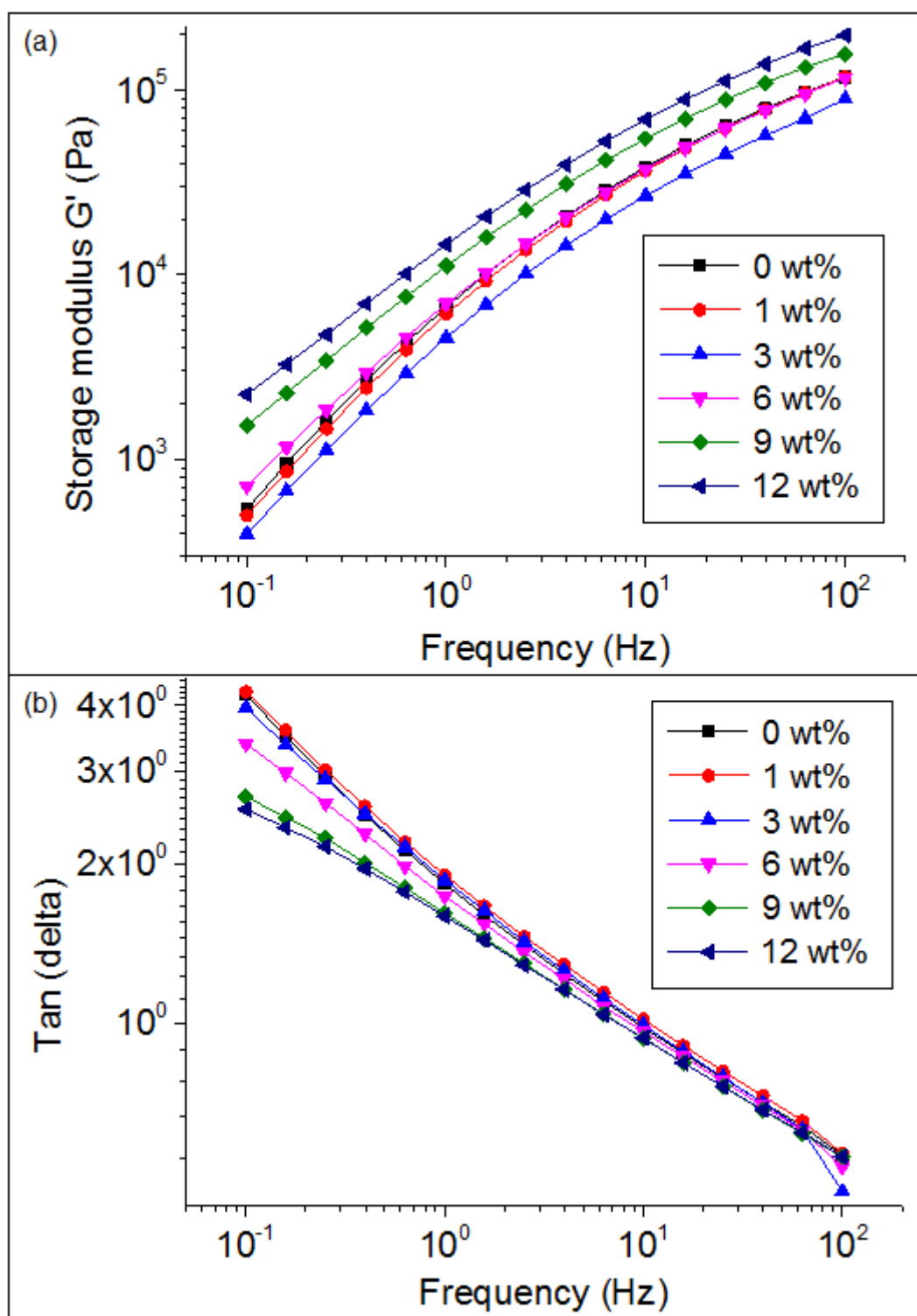


Figure S7. (a) Storage modulus (G') as a function of frequency for PP/Mg₃Al LDH nanocomposites. (b) Mechanical loss factor ($\tan \delta$) of as a function of frequency for PP/Mg₃Al-LDH nanocomposites.

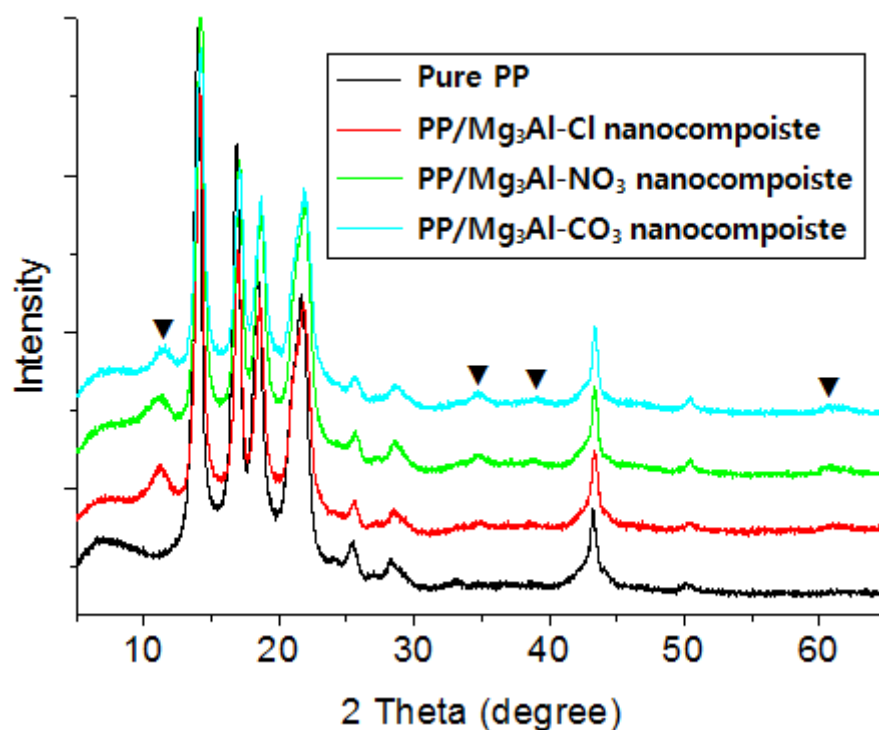


Figure S8. XRD analyses of pure PP, PP/Mg₃Al-Cl, PP/Mg₃Al-NO₃, PP/Mg₃Al-CO₃ nanocomposites; (▼) LDH.

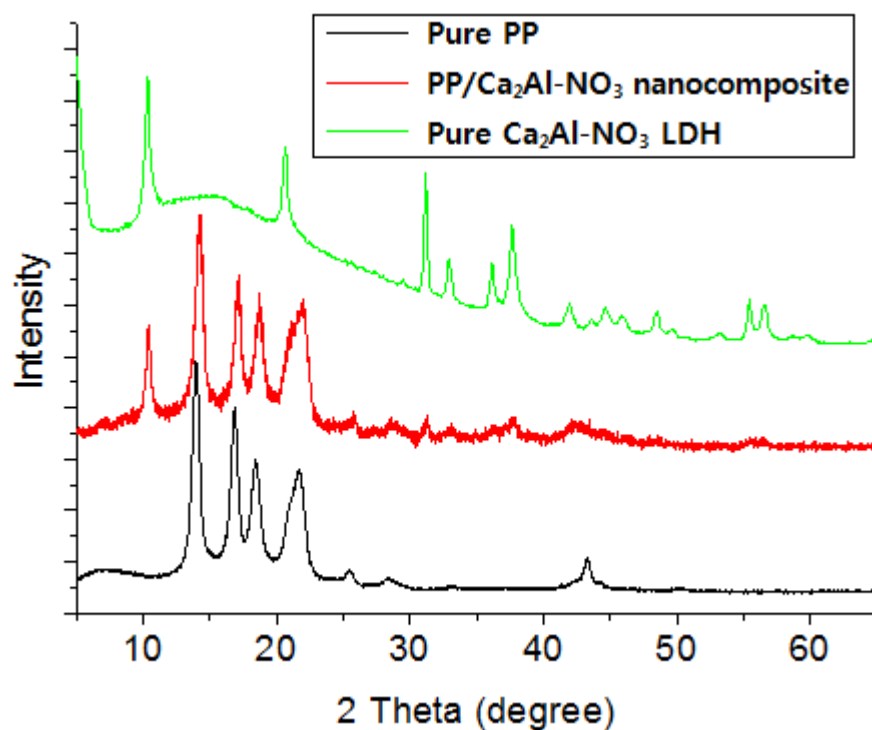


Figure S9. XRD analyses of pure PP, PP/Ca₂Al-NO₃ nanocomposite, and pure Ca₂Al-NO₃ LDH.

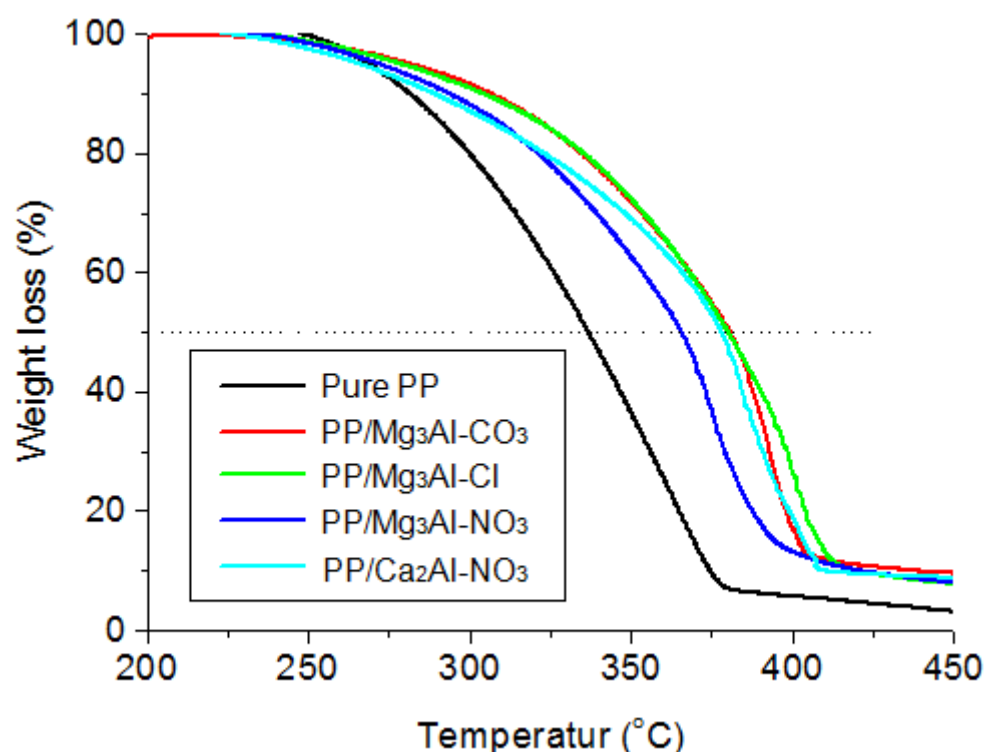


Figure S10. TGA analysis of Pure PP, PP/Mg₃Al-CO₃, PP/Mg₃Al-Cl, PP/Mg₃Al-NO₃, and PP/Ca₂Al-NO₃ LDH nanocomposites in air.